Optics and Lasers in Engineering 141 (2021) 106569

Contents lists available at ScienceDirect

Optics and Lasers in Engineering

journal homepage: www.elsevier.com/locate/optlaseng

Optical information hiding with non-mechanical ptychography encoding

Rui Ma [a], Yuan Li [a], Huizhu Jia [a], Yishi Shi [b,*], Xiaodong Xie [a], Tiejun Huang [a]

[a] School of Electronics Engineering and Computer Science, Peking University, Beijing, China
[b] Center for Materials Science and Optoelectronics Engineering, University of Chinese Academy of Sciences, Beijing, Chinas

ARTICLE INFO

Keywords:
Optical information hiding
Ptychography
Experiment

ABSTRACT

Since the ptychographic encoding can transform the secret information into series of diffractive patterns optically, it achieves the high security for information hiding. However, traditional ptychographic encoding requires the mechanical movements of the illuminated probe or the hidden object, which accumulates the errors greatly reducing the decoding quality. The errors have been reduced with the way of the single-shot ptychographic encoding, while its reliability and the decoding quality are still unideal. To solve these problems, we propose a non-mechanical ptychography to hide optical information for the first time. The core of this method includes both the non-mechanical ptychographic encoding (NPE) via a spatial light modulator and the decoding algorithm constrained with the phase-only quick respond code (PQR). NPE completely eliminates the errors arising from the ptychographic scanning, and the PQR-constrained decoding algorithm enables the high-quality information extracted from even only a few embedded diffractive patterns. The optical experiments verify that the method can achieve satisfactory robustness performance with the high repeatability, real-time encoding speed and the excellent information fidelity.

1. Introduction

Optical information security has become an active research field and attracted considerable researchers' attention in recent two decades. The main techniques proposed previously were random phase encoding [1,2,3,4], fractional Fourier transformation [5,6], ptychography [7,8,9], computational ghost imaging [10,11,12,13], chaotic mapping [14], visual cryptography [15,16], interference [17,18,19,20,21], computer-generated hologram [22], phase retrieval method [23], polarization encoding [24], hybrid methods [25], binary encoding [26], virtual optics [27], metasurface [28,29] and recently neural network [30,31]. Optical approaches, compared with digital approaches, usually have the advantages of parallel high-speed processing, multidimensional capabilities, and the large information capacity [32]. Therefore, this method is often used for security issues such as manipulation, information transfer, unauthorized access, and so on.

Ptychography is a powerful imaging method and attracts great attention[33,34,35]. Recently, we first proposed the ptychography-based optical image cryptosystem [7], which achieves improved security and feasibility. And then, we proposed the traditional ptychographic encoding (TPE) and used it for 3D information hiding [8]. Furthermore, we proposed the single-shot ptychographic encoding (SPE) attaining the optical watermarking [9]. However, the TPE requires mechanical movements that decrease system reliability and encoding efficiency. In addition, the SPE experimental system is complex and has poor repeatability. Thus, we propose the strategy of non-mechanical ptychography encoding (NPE), solving the problems both TPE and SPE and improving the reliability, security, and encoding efficiency. In Traditional ptychographic encoding (TPE), we need to laterally move the aperture to illuminate the object's different parts that overlap with each other, maintaining the position of the object; or, we laterally move the object keeping the aperture. In any case, the mechanical movement of the object or the aperture is unavoidable in the TPE-based system. In the NPE, the information is pre-encoded as a QR code and loaded onto a phase-only SLM. And then the QR code is encoded into the diffraction patterns by NPE. The illumination probe only illuminates a portion of the QR code on the SLM at a time, so it can ensure that each diffraction pattern contains only a portion of the information of the QR code. Hence, the hidden information will not be disclosed if the single diffraction pattern is cracked. Otherwise, phase information is more privacy because it is more difficult to reconstruct phase than amplitude. And the CCD can't detect the phase of wave-front directly, which shows that the phase has good imperceptibility. Therefore, phase is suitably utilized for the purpose of hiding. In addition, the ample structure parameters (λ, *d, translation-distance, pixel-size of CCD*) and diversity algorithm parameters (compression ratio, scrambling mode, attenuation coefficient, size of diffraction pattern) can obviously increase the richness of secret key. We have performed optical experiment and numerical simulation to demonstrate the above features of NPE-based optical hiding system.

* Corresponding author
E-mail address: optsys@gmail.com (Y. Shi).

https://doi.org/10.1016/j.optlaseng.2021.106569
Received 10 November 2020; Received in revised form 10 January 2021; Accepted 3 February 2021
Available online 18 February 2021

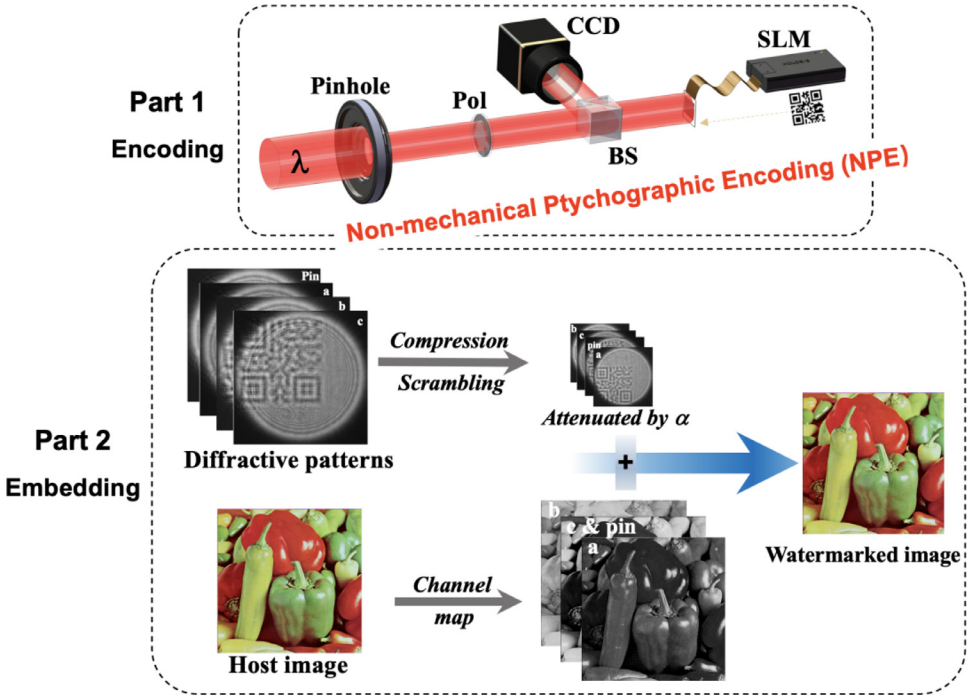

Fig. 1. Principle of optical information hiding by using non-mechanical ptychographic encoding (NPE). Part 1 is encoding, and part 2 is embedding.

2. Theory

2.1. System description

Fig. 1 shows the schematic of the principle of non-mechanical ptychographic encoding, which can be divided into two parts. Part 1 is an optical encoding system. Part 2 is performed to embed the diffraction pattern into the host image. In part 1, while either the pinhole or the QR codes are not necessary to be mechanically moved, the core overlapping requirement of ptychography can also be satisfied. The incident light first passes through the pinhole, and then transmits to the SLM through the polarizer (POL) and beam splitter (BS). The Pol and Pinhole are used to restrict the phase-only change of SLM and illuminate the fixed region of SLM, respectively. The wavelength of the laser is λ, and the diffraction distance from SLM to CCD is d. The wave-front modulated by SLM is propagated to BS and then incident to CCD to obtain the corresponding diffraction pattern. Encode the information into QR codes and load it into SLM. In the process of image acquisition, there are only three diffraction patterns of QR codes for ptychography. The frame rates of CCD and SLM are both 60/s, so we can turn 20 QR code into corresponding diffraction patterns per second. Each QR code containing different information needs to be loaded 3 times at different positions of the SLM in order to extract the information using ptychography algorithm. In this way, the NPE can encode 6 QR codes per second. In addition, we only need to collect the diffraction pattern of Pinhole once at the beginning. This shows the real-time nature of our proposed hidden system. In part 2, we embed the diffraction pattern of QR codes into the three channels of host image. Firstly, the diffraction pattern is compressed through the compression encoding method. Secondly, the compressed images are scrambled in a certain order. Thirdly, the encoded image is attenuated by α. Finally, the attenuated images are embedded into the three channels of host image, respectively.

Fig. 3 shows a flow chart of information hiding and extraction. The information that needs to be hidden is encoded into the corresponding QR code by computer, and the fault tolerance rate of QR code is 7%. Here we take hiding only one QR code as an example. According to the order of diffraction pattern acquisition in ptychographic imaging, three QR codes are loaded on the SLM in turn. One QR code needs to be loaded on the SLM three times in a row. At the same time, it needs to ensure that the area of image loaded each time is the area illuminated by the probe, and the position of image on SLM has a certain overlap. In addition, only part of the QR code is in the area illuminated by the probe when each time the QR code is loaded. Therefore, avoid information leakage caused by the single diffraction pattern of QR code appearing completely in the area illuminated by the probe.

2.2. Information encoding algorithm

The main parts of information hiding algorithm are as follows: QR code, compress, scramble, attenuate, and embed. Then we can obtain the host image with information to be transmitted. The process of embedding diffraction patterns is a blind watermarking technique in spatial domain. And the above five parts can be numerically expressed as six steps:

1) A plane wave with collimated and expanded are illuminated on the SLM after passing through the polarizer, pinhole and BS, these consecutive beams can be denoted $P(x, y)$.
2) Assume that the information function is $o(Inf)$, and $g[\cdot]$ denotes coding information into QR code. We can get the Q(QR code) loaded on the SLM:

$$Q(x, y) = g[o(Inf)] \tag{1}$$

3) We can get the wavefront reflected from the SLM:

$$U = P(x, y) \cdot Q(x, y) \tag{2}$$

4) Loading QR code on the SLM, we can simultaneously acquire the corresponding diffraction pattern I_i on the CCD:

$$I_i = |\mathcal{F}\{U\}| \; i = pin, 1, \; 2, 3 \ldots J \tag{3}$$

Where $\mathcal{F}\{\cdot\}$ represents the beam propagation operator, I_i and J denote the intensity measured in detector plane and the numbers of diffraction pattern respectively.

1) The encoded image E is generated by the compression encoding and scrambling encoding of diffraction pattern I_i, as shown in part 2 of Figs.1.

$$E = scr\big(comp\big(I_i\big)\big) \tag{4}$$

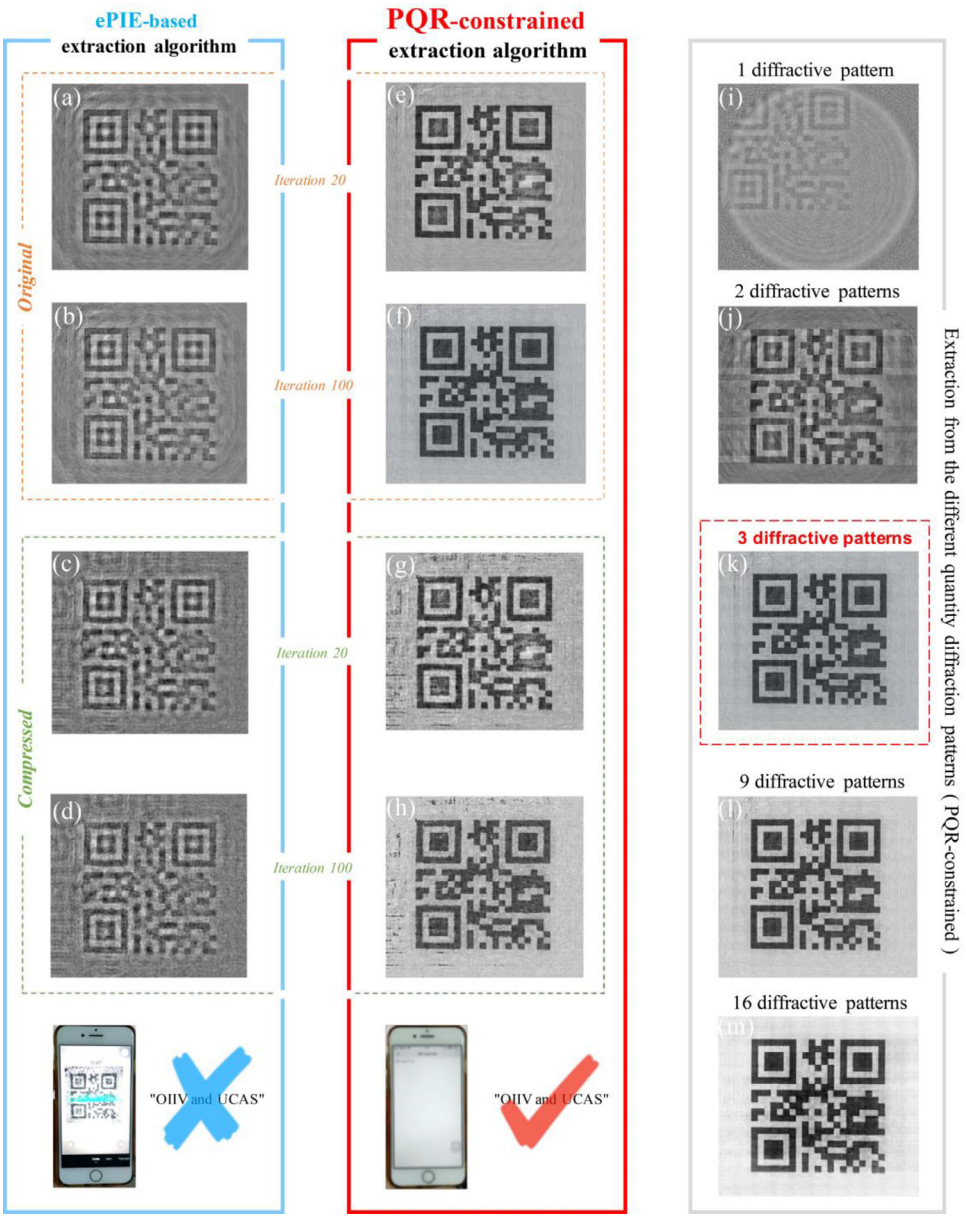

Fig. 2. Robustness comparison of experimental results for different extraction algorithms. (a)-(d) and (e)-(h) are the extracted results of iterations 20 and 100 by ePIE and PQR-constrained, respectively. (a)-(h) is all extracted from 3 diffractive patterns. (c), (d), (g), and (h) are the extracted results that compress 0.15 times to the diffraction patterns in encoding process, (a), (b), (e), and (f) are non-compression. (a), (e), (c), and (g) are the results iteration 20 using the extraction algorithm, (b), (f), (d), and (h) are the results iteration 100 using the extraction algorithm. (i)-(m) are extracted from 1, 2, 3, 9, and 16 diffractive patterns with non-compression by iterating 100 times PQR-constrained. The experiments results demonstrate that the 3 diffractive patterns are very adapted to encoding QR code for NPE. The 1 or 2 diffractive patterns are not enough for robustly extraction, and 9 or 16 diffractive patterns are too occupancy space to encoding appropriately.

Where $scr(\cdot)$ represents the compression encoding. Here, we use a simple nearest difference algorithm to compress the diffraction pattern directly. The symbol $comp(\cdot)$ indicates scrambling encoding, which is scrambling the order of the diffraction patterns.

1) The encoded image is embedded into three channels of the host image H in turn, using a blind watermarking technique in spatial domain:

$$T = E \cdot \alpha + H \tag{5}$$

Where α is attenuation coefficient, and T is the transmitted image.

2.3. Decoding algorithm by PQR-constrained

The extraction of information is the inversion of the encoding and hiding of information. Firstly, the diffraction pattern of QR code is extracted from the transmitted image faultlessly. Secondly, the diffraction pattern is arranged into the right size and order. Thirdly, the phase-only distribution of the QR code can be reconstructed by ePIE (extended ptychographical iterative engine). Finally, using smartphone to scan QR code to get hidden information. In the description below, the symbols $comp(\cdot)$ and $comp^{-1}(\cdot)$ respectively express the compression and decompression, symbol $scr(\cdot)$ and $scr^{-1}(\cdot)$ denote the scrambling and restoration of the order of the diffraction patterns respectively. The image T can be transmitted to any computer for decryption. The process of extracting and reconstructing the hidden information is as follows:

1) Extract the diffraction pattern E:

$$E = (T - H)/\alpha \tag{6}$$

2) Arrange E in the correct order, and then decompress these patterns:

$$I_i = comp^{-1}\left(scr^{-1}(E)\right) \tag{7}$$

3) Guess the phase-only value of the input QR code $Q(x, y)$, and calculate inverse Fresnel diffraction of the diffraction pattern I_{pin}:

$$P(x, y) = \left|\mathcal{F}^{-1}\left\{I_{pin}\right\}\right| \tag{8}$$

Then begin the following iterative process.

1) In the t^{th} iteration, $Q(x, y)$ is illuminated by the $(t-1)^{th}$ renewed probe, and the intensity ψ_t acquired at the output plane of NPE sys-

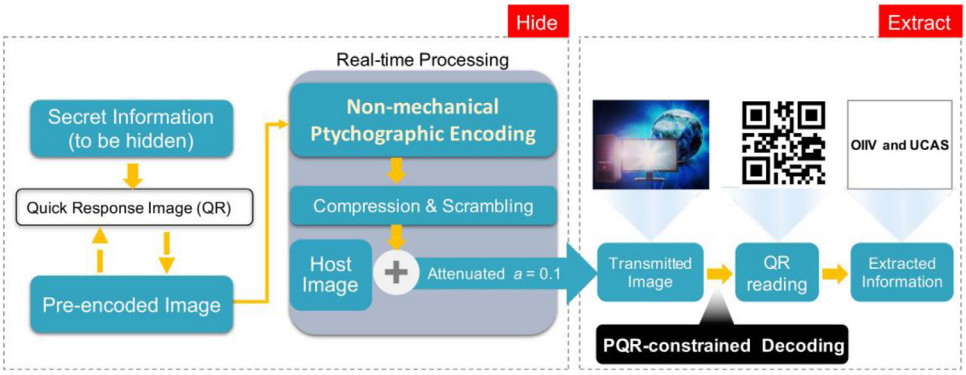

Fig. 3. Flow chart of NPE-based information hiding. On the left is the hidden process, and on the right is the extraction process.

tem:

$$U_t^i(x,y) = P_t^i(x,y) \cdot Q_t^i(x,y) \tag{9}$$

$$\psi_t^i = \mathcal{F}\left\{U_t^i(X,Y)\right\} \tag{10}$$

Where $U_t^i(x,y)$ denotes the exit wave at the position i and iteration t on the object plane.

1) Substitute the amplitude term of ψ_t^i with the detected pattern I_i, while preserving the phase:

$$\psi'^i_t = \sqrt{I_i} \cdot (\psi_t^i / |\psi_t^i|) \tag{11}$$

2) Back propagate the field ψ'^i_t to the SLM plane:

$$U'^i_t(x,y) = \mathcal{F}^{-1}\left\{\psi'^i_t\right\} \tag{12}$$

3) Update the object function and probe function using the following update equations:

$$Q_{t+1}^i(x,y) Q_t^i(x,y) + \beta_1 \cdot (P^{*i}_t(x,y) / \left|P_t^i(x,y)\right|^2_{max}) \cdot U'^i_t(x,y) - U_t^i(x,y) \tag{13}$$

$$P_{t+1}^i(x,y) = P_t^i(x,y) + \beta_2 \bullet \left(Q^{*i}_t(x,y)\right) / \left(\left|Q_t^i(x,y)\right|^2_{\max}\right) \bullet \left(U'^i_t(x,y) - U_t^i(x,y)\right) \tag{14}$$

Where the parameter β_1 and β_2 take the value 1.

1) Repeat the above steps 4 to 7 for the next object position $i+1$ until all scan positions have been reached to complete a single iteration.
2) Apply the binary constrain and phase-only constrain for the QR code to form a revised object estimate:

$$Q_t(x,y) = \begin{cases} \varepsilon \cdot \left(\mathrm{c} \cdot \dfrac{Q_t(x,y)}{|Q_t(x,y)|} + (1-\mathrm{c}) \cdot \chi\left\{\dfrac{Q_t(x,y)}{|Q_t(x,y)|}\right\}\right), & \mathrm{mod}(t,T) = 0 \\ Q_t(x,y), & \text{otherwise} \end{cases} \tag{15}$$

$$\chi\{a\} = \begin{cases} 1, & a > average\ (a) \\ 0, & a < average\ (a) \end{cases} \tag{16}$$

Where the parameter ε takes value 1 for phase-only constraints, and T=3 and c=0.9 are taken to avoid stagnation.

1) Calculate the peak signal to noise ratio (*PSNR*), which is used to evaluate the quality of the extracted QR code.

$$PANR = 10 \cdot log_{10}\left(MaxPV^2 / MSE\right)(dB) \tag{17}$$

$$MSE = \left(\sum_{m=1}^{M}\sum_{n=1}^{N}\left(\left(\phi_{m,n} - \phi'_{m,n}\right)^2\right)\right)/(M \cdot N) \tag{18}$$

where MSE is the mean squared error, $\phi_{m,n}$ and $\phi'_{m,n}$ are the original and the extracted images respectively. The size of $\phi_{m,n}$ and $\phi'_{m,n}$ are $M \cdot N$, and the maximum pixel value of the image is $MaxPV$.

1) After data reconstruction, the hidden information can be obtained by scanning the QR code.

3. Experimental results and analysis

As shown in Fig. 4, light source is a semiconductor laser with a wavelength of 532nm; pol is a polarizer used to guarantee phase-only modulation of SLM; pinhole1 and pinhole2 are apertures, and pinhole2 is an illumination probe to control the size of light spot on SLM; SLM is a German *holoeye* reflective phase-only spatial light modulator (model: pluto-vis-0 16-slm); CCD (charge coupled device) is the array product of *imperx* company (model: igv-b4020m-kf000), the pixel size is 9 μm, the array size is 4032 × 2688 pixel, the actual array size used is 888 × 888 pixels, the scanning mode is 3 × 3; the diffraction distance z = 185mm, PC is a computer connecting and controlling CCD and SLM at the same time. The overlap ratio is 87% in experiments and 64% in simulation. In this experiment, the beam generated by laser is adjusted into a parallel beam after passing through two mirrors, and the laser intensity is adjusted by CVF (circular variable filters) to meet the requirements of CCD acquisition, and the beam is expanded by filter and lens. After collimated and broadened, the plane wave beam will pass through pol and pinhole2 in turn to adjust the size of the probe, and then pass through BS to illuminate on SLM. After SLM modulation, the beam carrying information will be reflected back to BS, and then pass through BS to pol2. We will finally receive the diffraction pattern on CCD and transmit it to PC.

The optical information hiding system by non-mechanical ptychographic shown in Fig. 4. The information to be hidden is pre encoded to QR code. The information here can be text, number, etc. The hidden information in our experiment is “OIIV and UCAS”, the experimental setup is shown in Fig. 4(b), and the experimental flow chart and the extracted result are shown in Fig. 5.

The process of information hiding includes the following five steps. Firstly, information is encoded into a QR code. Secondly, it is recoded by an optical system. In this experiment, we chose 2 × 2 array scan mode. After adjusting the optical path, 4 diffraction patterns with the size of 888 × 888 pixels are received by CCD. As shown in Fig. 5, (a-d) are the positions of the QR code on the LCD of SLM, (a’-d’) are the relative positions of the probe on SLM, and (a”-d”) are the diffraction patterns corresponding to (a’-d’). Number the pictures in the order of collection. Thirdly, compress 4 diffractive patterns by 0.15 times, and randomly scramble the sequence number of pictures, and then we can obtain the scrambled diffraction patterns with 63 × 63 pixels in size. Fourth, the image is attenuated by the attenuation factor. Finally, the diffraction patterns are embedded in the three channels of the host image according to its sequence number. Because of the effective spatial compression of

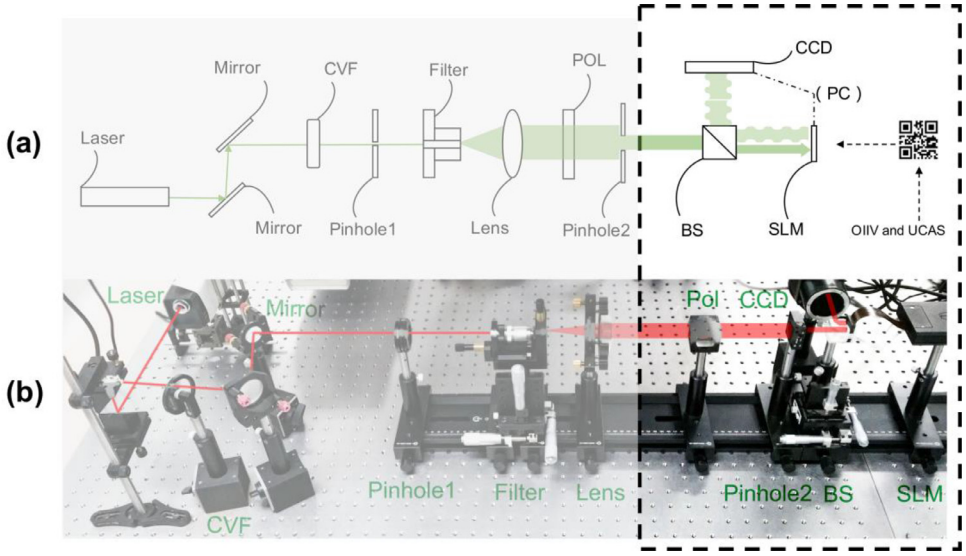

Fig. 4. Experimental setup of NPE-based information hiding. (a) is the abstract optical path, (b) is the actual experimental setup. The black dashed frame on the right is the core part of NPE, which contains BS, SLM, and CCD. The PC controls both SLM and CCD simultaneously to lode QR code and collect diffraction patterns.

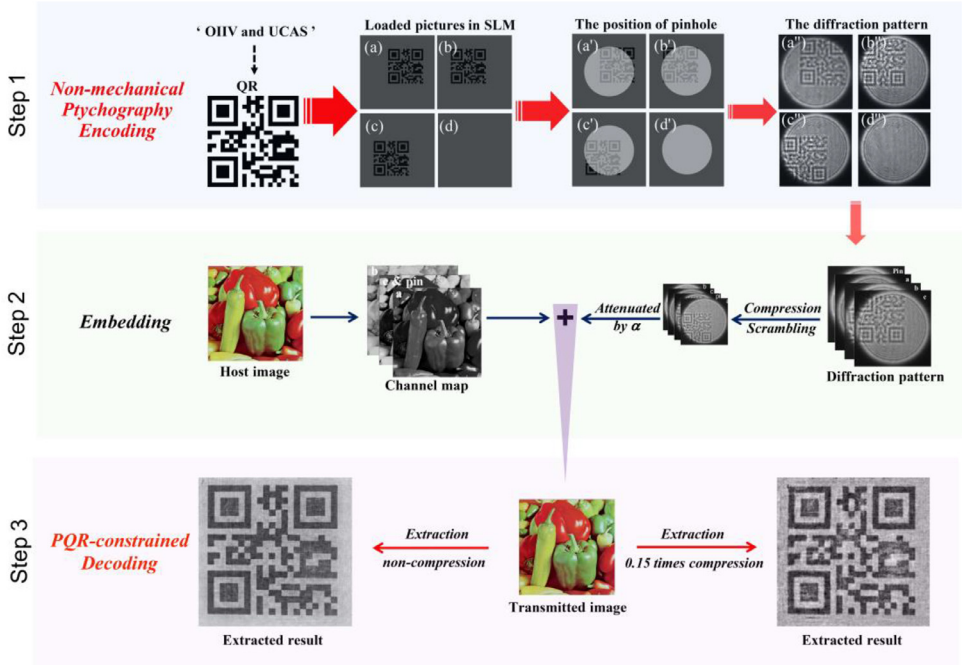

Fig. 5. Experimental demonstration of optical hiding NPE-based encoding. Step 1 is non-mechanical ptychographic encoding, and describes the acquisition of diffraction patterns. Step 2 is to embed the information into the host image, and step 3 is to extract and reconstruct the hidden information with and without compression.

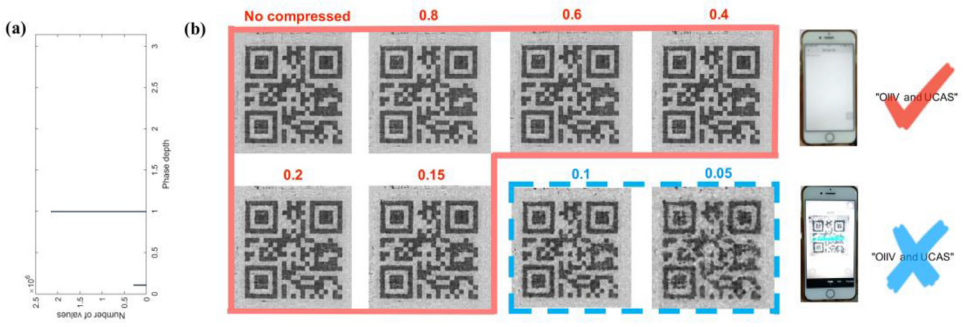

Fig. 6. Extraction results at different compression factors (Non-compression, 0.9, 0.8, …, 0.1, 0.05). (a) is the phase depth of the Fig. 5 (a-d) loaded on the SLM. (b) is the extracted from three diffraction patterns by iterating 100 times PQR-constrained when the compression factor changes. Hidden information "OIIV and UCAS" can be obtained from the QR code in the blue frame, but not from the red dashed box. We are using simply lossy compression. The optimal compression ratio is 0.15 and the maximum compression ratio is 0.1.

Table 1
PSNR of different attenuation coefficient α and schemes of encoding

***PSNR* (dB)**	Channel	With compression encoding	Without compression encoding
$\alpha = 0.1$	R	55.3547	41.4570
	G	52.0431	38.0513
	B	55.2884	41.2634
$\alpha = 0.15$	R	51.9961	38.1415
	G	48.5213	34.6840
	B	51.7666	37.7415
$\alpha = 0.2$	R	49.6654	35.8442
	G	46.0225	32.3371
	B	49.2678	35.3397
$\alpha = 0.3$	R	46.4704	32.7118
	G	42.6987	29.1145
	B	45.7460	32.1462

diffraction patterns and the strategy hidden in separate channels, it is no longer necessary to hide each diffraction image in multiple host images, which greatly saves the space occupied of the image and improves the efficiency of information transmission.

In the process of extraction, the results as shown in step 3 of Fig. 5 are extracted by the PQR-constrained iteration 20. We only used 3 diffractive patterns as the carrier of the hidden information in our experiment. This greatly reduces the time consumption due to the large amount of diffraction patterns. Therefore, in our hidden scheme, information extraction is much faster than traditional ePIE reconstruction. And the information extraction could be completed in 3 seconds (using CUDA parallel computing, Matlab-2019b). By combining with PQR-constrained, the extraction of hidden information is faster, which lays a foundation for the real-time and practical application of NPE.

In Fig. 5, the white numbers {pin, a, b, c} of the diffraction pattern in step 2 represents the order of collection. After compression and random scrambling, the order of diffraction patterns becomes {b, c & pin, a}, and the attenuation factor is 0.1. When extracting the information, any disorder of position for diffraction pattern will cause data reconstruction failure, unable to get effective QR code, and also unable to read the correct hidden information.

After the effective hiding of information, the next step is to analyze the extraction and reconstruction of hidden information. The security of NPE is given by the natural characteristics of ptychography imaging encoding. The location information, order, attenuation coefficient and compression ratio of each diffraction provides the security of the hiding system in varying degrees. In addition, the wavelength of the light source, the parameters of CCD and the diffraction distance of the optical imaging system also increase the security of the NPE system. In the process of extracting and reconstructing the hidden information, it is necessary to adjust the order and position of the diffraction pattern correctly to reconstruct the effective QR code. Finally, the hidden information of “OIIV and USAS” can be obtained by smartphone scanning.

4. Security of NPE-based optical hiding

In this section, we will analyze the security of NPE from three aspects: imperceptibility, scrambling encoding and diversity of structural parameters.

4.1. Imperceptibility

Imperceptibility is an important feature of optical information hiding, and also a crucial indicator of system security. In numerical simulation, the size of compressed diffraction pattern is half of the host image, which is 2240 × 2240 pixels. Under different attenuation coefficient, we embed the hidden information into three channels of host image, and calculate the corresponding channel peak signal to noise ratio (*PSNR)* between the hidden image and host image with and without compression encoding. In table 1, in order to demonstrate the high imperceptibility of hidden image, we test the value of *PSNR* with and without compression when $\boldsymbol{\alpha}$ is 0.1, 0.15, 0.2, 0.3, and the numerical of *PSNR* of each channel is given. The result of *PSNR* shows the strong imperceptibility of NPE-based hiding system.

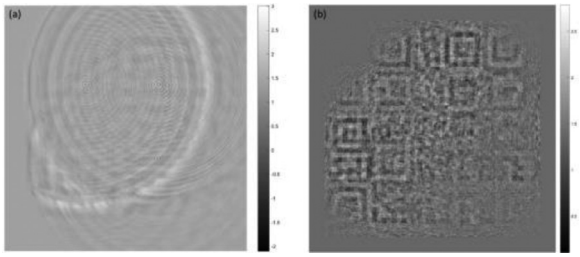

Fig. 7. Numerical and experimental demonstrations of the effectiveness of scrambling encoding. (a) Extracted phase map by numerical simulation; (b) Extracted phase map by experiment.

4.2. Scrambling encoding

Scrambling encoding is also a very effective way to enhance system security. In ptychography, each diffraction pattern corresponds to the position of acquisition one by one. We can’t reconstruct phase-only objects if the diffraction pattern and order of these maps are scrambled slightly, which small position errors will be spread to the whole region when the global updating of ptychography is carried out. In Fig. 7 (a) and (b), numerical simulation and experimental results demonstrate efficiency and feasibility of scrambling coding.

4.3. Diversity of structural parameters

The diversity of structural parameters (λ, *d, translation-distance, pixel-size of CCD*) can obviously increase the richness of secret key. In order to test the security of the structural parameters of hidden system, the numerical simulation has been performed. Fig. 8 (a)-(d) show the correlation index (*Co*) between extracted phase and actual QR code change under different structural parameters. The correct parameters λ is 632.8nm, *d* (diffraction distance) is 100mm, *translation-distance* is 297 pixels, and *pixel-size* is 5.5 μm. We only need to change one parameter and keep the other parameters correct during each simulation.

We can find that the *Co* are obviously more sensitive to *translation-distance* than λ, *d* and *pixel-size*. To get closer to the real optical system, we slightly change λ, *d, translation-distance*, and *pixel-size* simultaneously with λ=620 nm, *d*=110 mm, *translation-distance*=290 pixels, and *pixel-size=5.0* μm in numerical simulation, and the extracted QR code is shown as Fig. 9 (a). The changed experimental parameters are λ=620 nm, *d*=110 mm, *translation-distance*=300 pixels, and *pixel-size*=5.0 μm. Then, we can get the result as shown in the Fig. 9 (b), and the correct

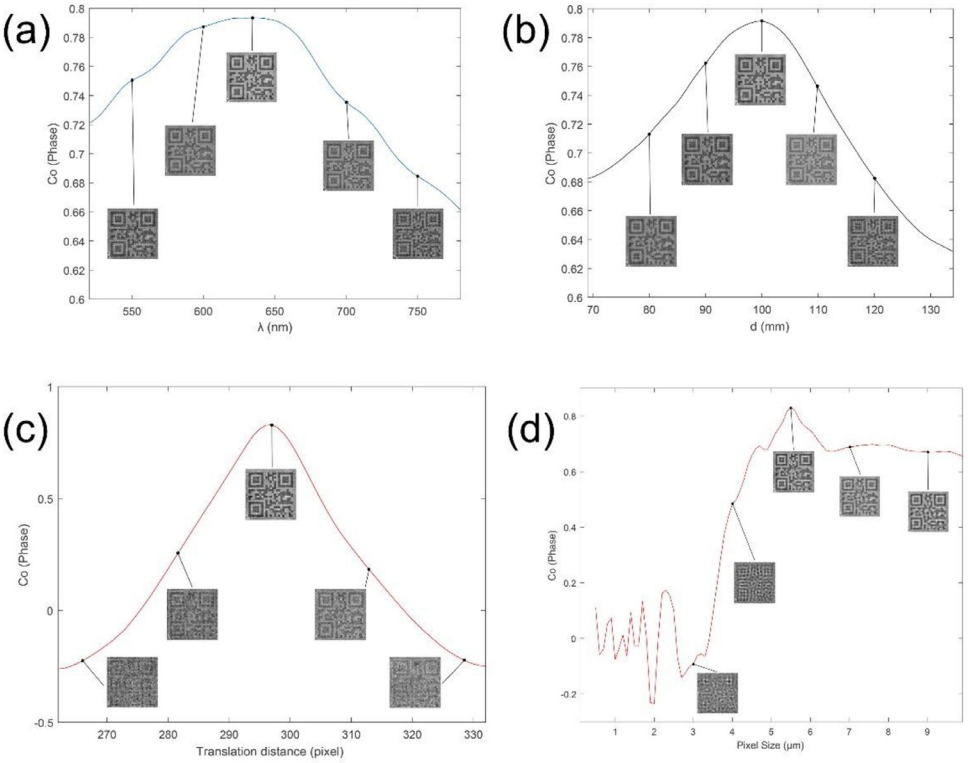

Fig. 8. The correlation coefficient *Co* curve of the extracted hidden QR code changes over the different structural parameters.

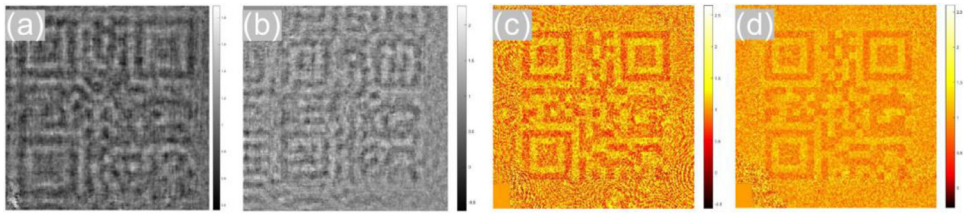

Fig. 9. Extracted QR code in different conditions. (a) is the numerical simulation result when the structural parameters change simultaneously, and (b) is the optical experimental result. (c) Extracted QR code under the attack of salt & pepper noise; (d) Extracted QR code under the attack of normalized random noise.

parameters are λ=632.8 nm, d=99 mm, *translation-distance*=279 pixels, and *pixel-size* =*5.5* μm. We cannot identify the hidden image when the diverse structural parameters have litter errors simultaneously. This shows that the structural parameters λ, *d, translation-distance* and *pixel-size* of NPE system are strong keys.

5. Robustness analysis

In this part, we test the robustness of NPE system against noise and occlusion attack, and give an optimized encoding scheme to enhance the robustness.

5.1. Numerical analysis

First, 0.3% salt and pepper noise and 3% normalized random noise are added to the transmission image, and the extracted QR code is shown in Fig. 9 (c) and (d), respectively. The reason is that the encoded image is a lossy compressed diffraction pattern, and the object to be reconstructed is a phase-only object, which is more difficult to recover than an amplitude object. In order to reduce the complexity of optical system and date reconstruction, only three diffraction patterns are used in ptychography.

Secondly, we demonstrate the robustness to occlusion attack. In our simulation, the occlusion attack will cause information loss of three channels in the occluded region. The transmitted images are occluded randomly by 1/8, and 1/16, respectively, as shown in Fig. 10(a) and (d). We assume that the size of the encoded image is half the host image. Fig. 10 (c) and (f) show the extracted phase, and Fig. 10 (b) and (e) show the extracted encoded image. When the occluded part is outside the hidden information area of transmitted image, the phase map of QR code can be identified. However, when there is diffraction information in the occluded region, the result of extracted will blurred.

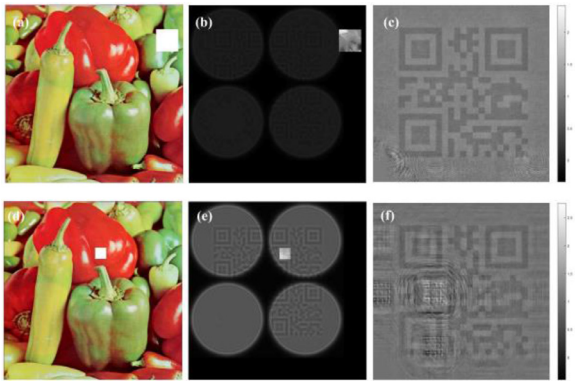

Fig. 10. Numerical results under attack of occlusion. (a) and (d) The transmitted images are occluded randomly by 1/8, and 1/16, respectively. (b) and (e) The extracted encoded image. (c) and (f) The extracted QR code.

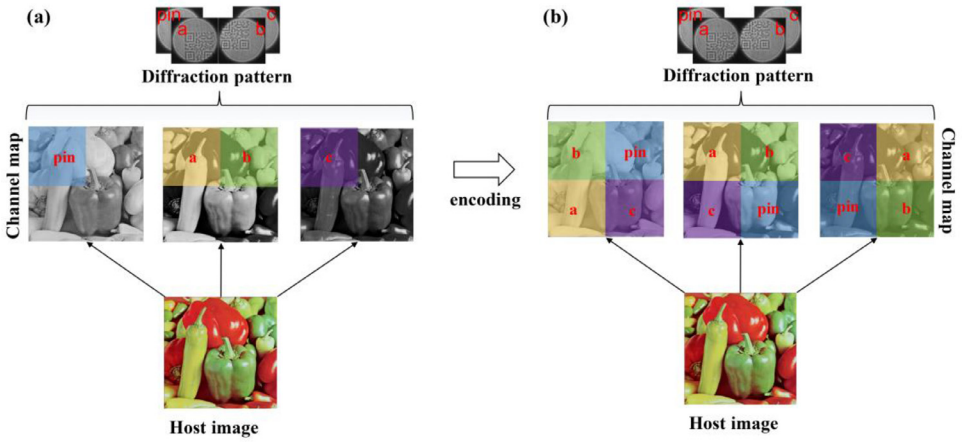

Fig. 11. Optimized scheme for enhance the robustness. (a) Original hidden scheme; (b) Optimized hidden scheme.

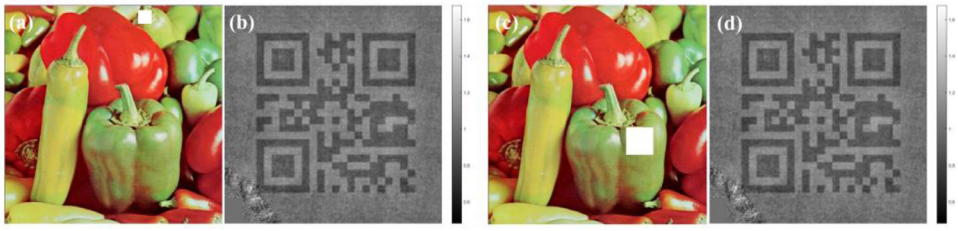

Fig. 12. Numerical results of optimized scheme under attack of occlusion. (a) and (c) The transmitted images are occluded randomly by 1/16, and 1/8, respectively. (b) and (d) The extracted QR code.

5.2. Optimization scheme

We propose an optimization scheme to improve the robustness of our hidden system. In numerical simulation, the encoded image is just constituted by 4 diffraction patterns, and the size of each one is half of the host image. Therefore, the occlusion attack has big destructiveness on the extracted quality when the occluded area contains hidden information. Inspired by three channels of color image, an optimized encoding scheme is proposed to improve the utilization of diffraction image. We encode the diffraction patterns with redundancy, and scramble all of the diffraction patterns with a predefined mode. Fig. 11(a) and (b) express original hidden scheme and optimized hidden scheme, respectively. We only hide information in part of the host image at the original hidden scheme, which is easy to attack by occlusion. As a result, each diffraction pattern will be used three times under the optimized hidden scheme, which can greatly improve the robustness of our method by increasing the redundant of diffraction date. As shown in Fig. 11 (b), as long as the occluded area is not very large, no matter which color area is attacked by occlusion, we can extract the non-attacked information from other channels. Hence, our method has strong robustness to occlusion attack. The optimized scheme described in Fig. 11(b). The QR code extracted under optimized scheme is shown in Fig. 12 (b) and (d).

6. Conclusions

In summary, we have demonstrated the security and robustness of the NPE, and applied NPE into information hiding successfully. First, this technique just needs to control the startup of the NPE on the computer without other mechanical operation, which makes the system quite simple and stable. Second, the extraction algorithm, PQR-constrained, greatly improves the fidelity of information and reduces the restriction to the number of diffraction patterns, which can perfectly save encoding time and space compared to TPE. Third, the phase-only QR code has high privacy and security, which means that NPE-based information hiding has strong imperceptibility. Moreover, the diversity of the structural parameters (λ, d, translation-distance, pixel-size) of the NPE form a large key space. Fourth, the NPE has excellent embed capacity and real-time due to the compressibility and efficient encoding strategy. Finally, an optimized encoding scheme based on spatial redundancy of host image color channel is proposed to enhance the robustness and security. Both the optical experiment and numerical simulation results denote the security and robustness of NPE.

Conflict of Interest

The authors declare that they have no known competing financial interests or personal relationships that could have appeared to influence the work reported in this paper.

Declaration of Competing Interest

The authors declare that they have no known competing financial interests or personal relationships that could have appeared to influence the work reported in this paper.

CRediT authorship contribution statement

Rui Ma: Conceptualization, Investigation, Methodology, Data curation, Software, Validation, Writing - original draft, Writing - review & editing. **Yuan Li:** Formal analysis, Funding acquisition. **Huizhu Jia:** Project administration. **Yishi Shi:** Funding acquisition, Investigation, Conceptualization. **Xiaodong Xie:** Supervision. **Tiejun Huang:** Supervision.

Acknowledgement

This work was supported by the Beijing Major Science and Technology Project (No. Z191100010618003); PKU-Baidu Fund (2019BD004); Innovation Promotion Association CAS (2017489); Youth Supported by the University of Chinese Academy of Sciences; Fusion Foundation of Research and Education of CAS; Natural Science Foundation of Hebei Province of China (F2018402285); National Natural Science Foundation of China (61575197); Funded Project of Hebei Province Innovation Capability Improvement Plan (No.20540302D); The Fundamental Research Funds for the Central Universities.

References

[1] Refregier P, Javidi B. Optical image encryption based on input plane and Fourier plane random encoding. Opt. Lett 1995;20(7):767–9.
[2] Wang R K, Watson I A, Chatwin CR. Random phase encoding for optical security. Opt. Eng 1996:35.
[3] Kishk S, Javidi B. Information hiding technique with double phase encoding. Appl. Opt. 2002;41:5462–70.
[4] He M, Tan Q, Cao L, He Q, Jin G. Security enhanced optical encryption system by random phase key and permutation key. Opt. Express 2009;17(25):22462–73.
[5] Unnikrishnan G, Joseph J, Singh K. Optical encryption by double-random phase encoding in the fractional Fourier domain. Opt. Lett 2000;25(12):887–9.
[6] Wang X, Chen W, Chen X. Fractional Fourier domain optical image hiding using phase retrieval algorithm based on iterative nonlinear double random phase encoding. Opt. Express 2014;22(19):22981–95.
[7] Shi Y, Li T, Wang Y, Gao Q, Zhang S, Li H. Optical image encryption via ptychography. Opt. Lett 2013;38(9):1425–7.
[8] Zhang J, Wang Z, Li T, Pan A, Wang Y, Shi Y. 3D object hiding using three-dimensional ptychography. J. Opt 2016;18:095701.
[9] Xu W, Xu H, Luo Y, Li T, Shi Y. Optical watermarking based on single-shot-ptychography encoding. Opt. Express 2016;24:27922–36.
[10] Wang L, Zhao S, Cheng W, Gong L, Chen H. Optical image hiding based on computational ghost imaging. Opt. Commun 2016;366:314–20.
[11] Liansheng S, Jiahao W, Ailing T, Asundi A. Optical image hiding under framework of computational ghost imaging based on an expansion strategy. Opt. Express 2019;27(5):7213–25.
[12] Zhang L, Zhang Z, Kang Y, Ye H, Xiong R, Yuan X, Wang Z, Wang K, Zhang D. Research on double-layers optical information encryption based on ghost imaging. Opt. Commun 2020;455:124585.
[13] Qu G, Meng X, Yin Y, Wu H, Yang X, Peng X, He W. Optical color image encryption based on Hadamard single-pixel imaging and Arnold transformation. Opt. Laser Eng 2021;137:106392.
[14] Liu Z, Zhang Y, Liu W, Meng F, Wu Q, Liu S. Optical color image hiding scheme based on chaotic mapping and Hartley transform. Opt. Laser Eng 2013;51(8):967–72.
[15] Shi Y, Yang X. Optical hiding with visual cryptography. J. Opt 2017;19(11):115703.
[16] Yang N, Gao Q, Shi Y. Visual-cryptographic image hiding with holographic optical elements. Opt. Express 2018;26(24):31995–2006.
[17] Kishk S, Javidi B. Watermarking of three-dimensional objects by digital holography. Opt. Lett 2003;28:167–9.
[18] Hamam H. Digital holography-based steganography. Opt. Lett 2010;35:4175–7.
[19] Yang B, Liu Z, Wang B, Zhang Y, Liu S. Optical stream-cipher-like system for image encryption based on Michelson interferometer. Opt. Express 2011;19:2634–42.
[20] He W, Peng X, Meng X. Optical multiple-image hiding based on interference and grating modulation. J. Opt 2012;14(7):075401.
[21] Wang X, Zhao D. Optical image hiding with silhouette removal based on the optical interference principle. Appl. Opt 2012;51(6):686–91.
[22] Kong D, Cao L, Shen X, Zhang H, Jin G. Image encryption based on interleaved computer-generated holograms. IEEE Transactions on Industrial Informatics 2017;14(2):673–8.
[23] Wang X, Zhao D. Double-image self-encoding and hiding based on phase-truncated Fourier transforms and phase retrieval. Opt. Commun 2011;284(19):4441–5.
[24] Tu H Y, Cheng C J, Chen ML. Optical image encryption based on polarization encoding by liquid crystal spatial light modulators. J. Opt A: Pure and Applied Optics 2004;6(6):524.
[25] Nomura T, Uota K, Morimoto Y. Hybrid optical encryption of a 3-D object using a digital holographic technique. Opt. Eng 2004;43(10):2228–33.
[26] Zhengjun Liu, Qing Guo, Lie Xu, Muhammad Ashfaq Ahmad, Shutian Liu. Double image encryption by using iterative random binary encoding in gyrator domains. Opt. Express 2010;18:12033–43.
[27] Kim H, Kim D H, Lee Y H. Encryption of digital hologram of 3-D object by virtual optics. Opt. Express 2004;12(20):4912–21.
[28] Walter Felicitas, Li G, Meier C, Zhang S, Zentgraf T. Ultrathin nonlinear metasurface for optical image encoding. Nano letters 2017(5):3171–5.
[29] Li J, Kamin S, Zheng G, Neubrech F, Zhang S, Liu N. Addressable metasurfaces for dynamic holography and optical information encryption. Science advances 2018(6):eaar6768.
[30] Gao Y, Jiao S, Fang J, Lei T, Xie Z, Yuan X. Multiple-image encryption and hiding with an optical diffractive neural network. Opt. Commun 2020:125476.
[31] Li J, Li Y, Li J, Zhang Q, Yang G, Chen S, Wang C, Li J. Deep-learning-based optical image hiding. arXiv preprint arXiv; 2020. p. 04130.
[32] Jiao S, Zhou C, Shi Y, Zou W, Li X. Review on optical image hiding and watermarking techniques. Opt. Laser Technology 2019;109:370–80.
[33] Ma R, Zhang S, Ruan T, Tao Y, Wang H, Yi Shi. Scanning-Position Error-Correction Algorithm in Dual-Wavelength Ptychographic Microscopy. Chinese Physics Letters 2020(4):044201.
[34] Ma R, Yang D, Yu T, Li T, Sun X, Zhu Y, Yang N, Wang H, Shi Y. Sharpness-statistics-based auto-focusing algorithm for optical ptychography. Opt. Laser Eng 2020;128:106053.
[35] Maiden A M, Rodenburg JM. An improved ptychographical phase retrieval algorithm for diffractive imaging. Ultramicroscopy 2009;109(10):1256–62.